iJRASET
International Journal For Research in Applied Science and Engineering Technology



INTERNATIONAL JOURNAL FOR RESEARCH

IN APPLIED SCIENCE & ENGINEERING TECHNOLOGY

Volume: 3 **Issue:** VII **Month of publication:** July 2015

DOI:

www.ijraset.com

Call: 08813907089 | E-mail ID: ijraset@gmail.com

Volume 3 Issue VII, July 2015
ISSN: 2321-9653
International Journal for Research in Applied Science & Engineering Technology (IJRASET)

Non-Linear FEA Analysis of a Drive Shaft Made Of Composite Material Using Ansys

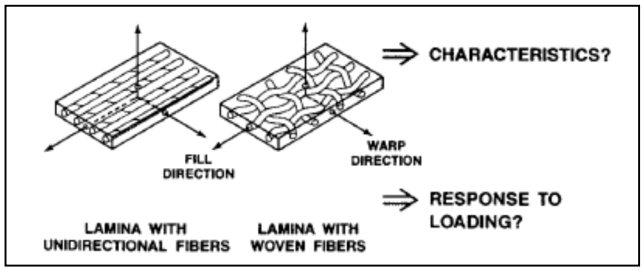
Amit Soni[1] Mr. Hari Ram Chandrakar[2]
[1]M.E. Final Year Student, [2]Assistant Professor, Mechanical Engineering,
Shankaracharya Technical Campus,
Shri Shankaracharya Group of Institutions (FET), Junuani, Bhilai, Chattishgarh.

Abstract*— an automobile drive shaft is used to transmit torque from the gear box to differential. A drive shaft is subjected to different types of loadings like bending load, torsional load, impact load and fatigue load. To survive under these loading a drive shaft has to have high module but at the same time mass of the drive shaft should not be high. These properties of material are readily found in composite materials. So it is very much advantageous in substituting drive shaft made of conventional isotropic or alloy material with composite material for its higher specific stiffness and strength. In the present work a drive shaft made of high modulus carbon/epoxy composite material in numerical software named ANSYS. Further the drive shaft has been tapered with different taper angle and then it has been simulated in ANSYS for buckling analysis and modal analysis. Lastly different results have been compared.

Keywords*— Composite materials, Drive shaft, E-Glass/Epoxy, HS Carbon/Epoxy, HM Carbon/Epoxy, Von-Misses Stress, Modal analysis

I. INTRODUCTION

A composite material or object is made of few material laminas together. Materialistic behaviour of a composite object depends on the properties of lamina and their orientation. Regarding macro mechanics the basic questions are: (1) what are the characteristics of a lamina? And (2) how does a lamina respond to applied stresses as in fig. 1. A lamina is a flat (or curved as in a shell) arrangement of unidirectional or woven fibres in a supporting matrix. The concepts developed in this chapter apply equally to both types of lamina is the basic building block in laminated fibre reinforced composite materials. Thus, knowledge of the mechanical behaviour of a lamina is essential to the understanding of laminated fiber-reinforced structures. This topic is focused on macro mechanical behaviour, i.e., the behaviour when only averaged apparent mechanical properties are considered, rather than the detailed interactions of the constituents of the composite material. The basic restriction for this discussion is to linear elastic behaviour. Both stiffnesses and strengths have been discussed for complex through simple materials in what follows.



A. Stress-Strain Relations For Plane Stress In An Orthotropic Material

For a unidirectional reinforced lamina in the 1-2 planes as shown in fig. 2 or a woven lamina as in Fig 1, a plane stress state is defined by setting

$$\sigma_3 = 0 \qquad \tau_{23} = 0 \qquad \tau_{31} = 0 \qquad (1)$$

so that

$$\sigma_1 \neq 0 \qquad \sigma_2 \neq 0 \qquad \tau_{12} \neq 0 \qquad (2)$$

in the three-dimensional stress-strain relations for anisotropic, monoclinic, orthotropic, transversely isotropic, or isotropic materials.

©IJRASET 2015: All Rights are Reserved

Volume 3 Issue VII, July 2015
ISSN: 2321-9653
International Journal for Research in Applied Science & Engineering Technology (IJRASET)

The practical and achievable objective is to know how we should use a lamina with fibres in its plane after identifying plane stress state on a lamina. Load on a lamina should always be in the direction of fibre because lamina cannot withstand high stresses in any direction other than that of the fibres so carrying in-plane stresses is its fundamental capability. Load in other planes cannot be beard by a unidirectional reinforced lamina and to do so fibre reinforcement in that direction is needed. Thus, a laminate is needed, but we concentrate on the characteristics of a lamina in this chapter. Practical examples of in-plane loaded structural elements are most car body panels, aircraft wings and fuselages, etc.

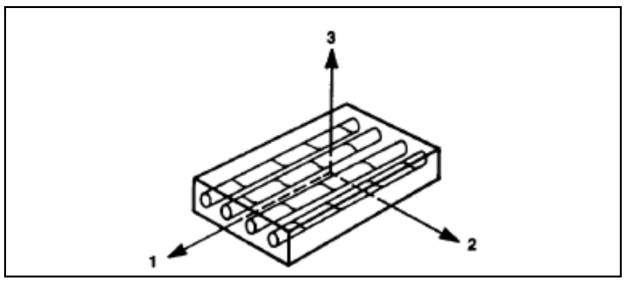


Fig. 2: Unidirectional Reinforced Lamina

For orthotropic materials, imposing a state of plane stress results in implied out-of-plane strains of

$$\varepsilon_3 = S_{13}\sigma_1 + S_{23}\sigma_2 \quad \gamma_{23} = 0 \quad \gamma_{31} = 0 \quad (3)$$

where

$$S_{13} = -\frac{\nu_{13}}{E_1} = -\frac{\nu_{31}}{E_3} \qquad S_{23} = -\frac{\nu_{23}}{E_2} = -\frac{\nu_{32}}{E_3} \quad (4)$$

Moreover, the strain-stress relations reduce to

$$\begin{bmatrix}\varepsilon_1\\ \varepsilon_2\\ \gamma_{12}\end{bmatrix} = \begin{bmatrix}S_{11} & S_{12} & 0\\ S_{12} & S_{22} & 0\\ 0 & 0 & S_{66}\end{bmatrix}\begin{bmatrix}\sigma_1\\ \sigma_2\\ \tau_{12}\end{bmatrix} \qquad (5)$$

Supplemented by eq. (3) where

$$S_{11} = \frac{1}{E_1} \qquad S_{11} = -\frac{\nu_{12}}{E_1} = -\frac{\nu_{21}}{E_2} \qquad S_{22} = \frac{1}{E_2} \qquad S_{66} = \frac{1}{G_{12}} \quad (6)$$

Note that in order to determine ε_3 in eq. (3), ν_{13} and ν_{23} must be known in addition to the engineering constants in eq. (6). That is ν_{13} and ν_{23} arise form S_{13} and S_{23} in eq. (3).

The strain-stress relations in eq. (5) can be inverted to obtain the stress-strain relations

$$\begin{bmatrix}\sigma_1\\ \sigma_2\\ \tau_{12}\end{bmatrix} = \begin{bmatrix}Q_{11} & Q_{12} & 0\\ Q_{12} & Q_{22} & 0\\ 0 & 0 & Q_{66}\end{bmatrix}\begin{bmatrix}\varepsilon_1\\ \varepsilon_2\\ \gamma_{12}\end{bmatrix} \qquad (7)$$

Where the Q_{ij} are the so-called reduced stiffnesses for a plane stress state in the 1-2 plane which are determined either (3) as the components of the inverted compliance matrix in eq. (5) or (4) from the C_{ij} directly by applying the condition $\sigma_3 = 0$ to the strain-stress relations to get an expression for ε_3 and simplifying the results to get

$$Q_{ij} = C_{ij} - \frac{C_{i3}C_{j3}}{C_{33}} \qquad i,j = 1,2,6 \qquad (8)$$

The term C_{63} is zero because no shear-extension coupling exists for an orthotropic lamina in principal material coordinates. For the orthotropic lamina, the Q_{ij} are

$$Q_{11} = \frac{S_{22}}{S_{11}S_{22} - S_{12}^2} \qquad Q_{22} = \frac{S_{11}}{S_{11}S_{22} - S_{12}^2}$$

©IJRASET 2015: All Rights are Reserved

Volume 3 Issue VII, July 2015
ISSN: 2321-9653
International Journal for Research in Applied Science & Engineering Technology (IJRASET)

$$Q_{12} = \frac{S_{12}}{S_{11}S_{22} - S_{12}^2} \qquad Q_{66} = \frac{1}{S_{66}} \qquad (9)$$

or, in terms of the engineering constants,

$$Q_{11} = \frac{E_1}{1 - \nu_{12}\nu_{21}} \qquad Q_{22} = \frac{E_2}{1 - \nu_{12}\nu_{21}}$$
$$Q_{12} = \frac{\nu_{12}E_1}{1 - \nu_{12}\nu_{21}} = \frac{\nu_{21}E_1}{1 - \nu_{12}\nu_{21}} \qquad Q_{66} = G_{12} \quad (10)$$

Note that there are four independent material properties, E_1, E_2, ν_{12} and G_{12}, in equations (5) and (7) when equations (6) and (10) are considered in addition to the reciprocal relation

$$\frac{\nu_{12}}{E_1} = \frac{\nu_{21}}{E_2} \qquad (11)$$

The preceding stress-strain and strain-stress relations are the basis for stiffness and stress analysis of an individual lamina subjected to forces in its own plane. Thus, the relations are indispensable in laminate analysis.

For plane stress on isotropic materials, the strain-stress relations are

$$\begin{bmatrix}\varepsilon_1\\ \varepsilon_2\\ \gamma_{12}\end{bmatrix} = \begin{bmatrix}S_{11} & S_{12} & 0\\ S_{12} & S_{22} & 0\\ 0 & 0 & 2(S_{11} - S_{12})\end{bmatrix}\begin{bmatrix}\sigma_1\\ \sigma_2\\ \tau_{12}\end{bmatrix} \qquad (12)$$

where

$$S_{11} = \frac{1}{E} \qquad S_{12} = -\frac{\nu}{E} \qquad (13)$$

And the stress-strain relations are

$$\begin{bmatrix}\sigma_1\\ \sigma_2\\ \tau_{12}\end{bmatrix} = \begin{bmatrix}Q_{11} & Q_{12} & 0\\ Q_{12} & Q_{11} & 0\\ 0 & 0 & Q_{66}\end{bmatrix}\begin{bmatrix}\varepsilon_1\\ \varepsilon_2\\ \gamma_{12}\end{bmatrix} \qquad (14)$$

where

$$Q_{11} = \frac{E}{1 - \nu^2} \qquad Q_{12} = \frac{\nu E}{1 - \nu^2} \qquad Q_{66} = \frac{E}{2(1 + \nu)} \quad (15)$$

The preceding isotropic relations can be obtained either from the orthotropic relations by equating E_1 to E_2 and G_{12} to G or by the same manner as the orthotropic relations were obtained.

Observing the physical symmetry of the fibers and matrix in a unidirectional reinforced lamina enables us to deduce how some of the out-of-plane properties are related to the in-plane properties, E1, E2, v12, and G12. Consider the cube-shaped portion of a unidirectional reinforced lamina in principal material coordinates in fig. 4.8. First, E3 = E2 because both stiffnesses are measured across fibres in the same manner. That is, in general, the 3-direction can be treated just as if it were the 2-direction for a unidirectional reinforced lamina. Second, v31 = v21 (hence, v13 = v12) for the same reason. Third, irrespective of whether the shear stress τ13 or τ12 is applied, the resulting deformations are identical because, by symmetry, the fibres have the same orientation to the applied shearing stress, so G13 = G12. Even if the fibre distribution in the 2-3 planes of the cube in fig. 3 were random, the same conclusions would apply. That is, with either the fiber-spacing regularity in fig. 4 or random fibre distribution in the 2-3 plane, the 2-3 plane can be regarded as a plane of isotropy because all stiffnesses, E, in the plane are the same. When we account for the different E1 from E2 in the 1-2 plane, we recognize that the lamina is a transversely isotropic material in three dimensions. However, when we concentrate only on the 1-2 plane, we call the lamina orthotropic. If the lamina is compacted in the 3-direction during the curing process, then slight differences in the properties between the 2- and 3-directions would result, and the material would be orthotropic in the three-dimensional sense.

©IJRASET 2015: All Rights are Reserved

Volume 3 Issue VII, July 2015
ISSN: 2321-9653
International Journal for Research in Applied Science & Engineering Technology (IJRASET)

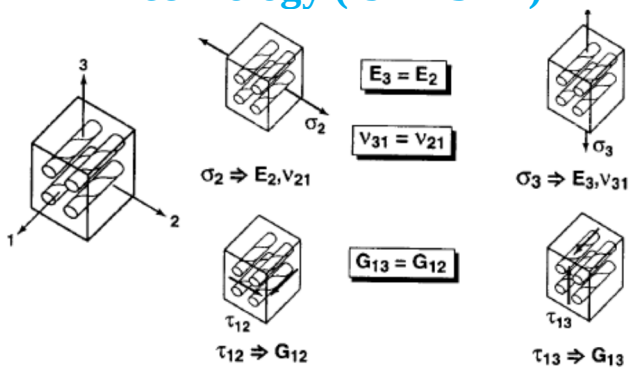


Fig. 3: Physical Symmetry of a Unidirectional Reinforced Lamina

A. Stress-Strain Relation For A Lamina Of Arbitrary Orientation

For an orthotropic material as we discussed in previous section the stresses and strain were defined in the principal material coordinates. The geometrically natural solution of the problem does not coincide with the principal directions of orthotropic. For example, consider the helically wound fibre-reinforced circular cylindrical shell in fig. 4.9. there, the coordinates natural to the solution of the shell problem are the shell coordinates x, y, z, whereas the principal material coordinates are x', y', z'. Other examples include laminated plates with different lamina at different orientations. Thus a relation is needed between the stresses and strains in the principal material coordinates and those in the body coordinates. Then, a method of transforming stress-strain relations from one coordinate system to another is also needed.

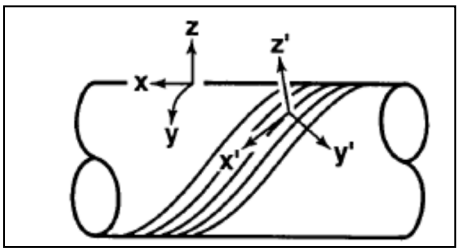


Fig. 4: Helically Wound Fibre-Reinforced Circular Cylindrical Shell

At this point, we recall from elementary mechanics of materials the transformation equations for expressing stresses in an x-y coordinate system in terms of stresses in a1-2 coordinate system,

$$\begin{bmatrix}\sigma_x\\ \sigma_y\\ \tau_{xy}\end{bmatrix} = \begin{bmatrix}\cos^2\theta & \sin^2\theta & -2\sin\theta\cos\theta\\ \sin^2\theta & \cos^2\theta & \sin\theta\cos\theta\\ \sin\theta\cos\theta & -\sin\theta\cos\theta & \cos^2\theta-\sin^2\theta\end{bmatrix}\begin{bmatrix}\sigma_1\\ \sigma_2\\ \tau_{12}\end{bmatrix} \quad (16)$$

Where, θ is the angle from the x-axis to the 1-axis (fig. 3). Note especially that the transformation has nothing to do with the material properties but is merely a rotation of stress directions. Also, the direction of rotation is crucial.

Similarly, the strain-transformation equations are

$$\begin{bmatrix}\varepsilon_x\\ \varepsilon_y\\ \frac{\gamma_{xy}}{2}\end{bmatrix} = \begin{bmatrix}\cos^2\theta & \sin^2\theta & -2\sin\theta\cos\theta\\ \sin^2\theta & \cos^2\theta & \sin\theta\cos\theta\\ \sin\theta\cos\theta & -\sin\theta\cos\theta & \cos^2\theta-\sin^2\theta\end{bmatrix}\begin{bmatrix}\varepsilon_1\\ \varepsilon_2\\ \frac{\gamma_{12}}{2}\end{bmatrix} \quad (17)$$

©IJRASET 2015: All Rights are Reserved

Volume 3 Issue VII, July 2015
ISSN: 2321-9653
International Journal for Research in Applied Science & Engineering Technology (IJRASET)

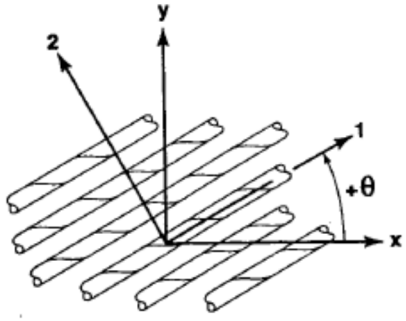


Fig. 5 Positive Rotation of Principal Material Axes from x-y Axes

Where we observe that strains do transform with the same transformation as stresses if the tensor definition of shear is used (which is equivalent to dividing the engineering shear strain by two).

The transformations are commonly written as

$$\begin{bmatrix}\sigma_x\\ \sigma_y\\ \tau_{xy}\end{bmatrix} = [T]^{-1}\begin{bmatrix}\sigma_1\\ \sigma_2\\ \tau_{12}\end{bmatrix} \qquad \ldots\ldots\ldots\ldots (18)$$

$$\begin{bmatrix}\varepsilon_x\\ \varepsilon_y\\ \frac{\gamma_{xy}}{2}\end{bmatrix} = [T]^{-1}\begin{bmatrix}\varepsilon_1\\ \varepsilon_2\\ \frac{\gamma_{12}}{2}\end{bmatrix} \qquad \ldots\ldots\ldots\ldots (19)$$

where the superposition -1 denotes the matrix inverse and

$$[T] = \begin{bmatrix}\cos^2\theta & \sin^2\theta & 2\sin\theta\cos\theta\\ \sin^2\theta & \cos^2\theta & -\sin\theta\cos\theta\\ -\sin\theta\cos\theta & \sin\theta\cos\theta & \cos^2\theta-\sin^2\theta\end{bmatrix} \qquad (20)$$

However, if the simple matrix

$$[R] = \begin{bmatrix}1 & 0 & 0\\ 0 & 1 & 0\\ 0 & 0 & 2\end{bmatrix} \qquad (21)$$

due to Reuter [2-4] is introduced, then the engineering strain vectors

$$\begin{bmatrix}\varepsilon_1\\ \varepsilon_2\\ \gamma_{12}\end{bmatrix} = [R]\begin{bmatrix}\varepsilon_1\\ \varepsilon_2\\ \frac{\gamma_{12}}{2}\end{bmatrix} \qquad (22)$$

$$\begin{bmatrix}\varepsilon_1\\ \varepsilon_2\\ \gamma_{xy}\end{bmatrix} = [R]\begin{bmatrix}\varepsilon_1\\ \varepsilon_2\\ \frac{\gamma_{xy}}{2}\end{bmatrix} \qquad (23)$$

can be used instead of the tensor strain vectors in the strain transformations as well as in stress-strain law transformations. The beauty of Reuter's transformation is that concise matrix notation can then be used. As a result, the ordinary expressions for stiffness and compliance matrices with awkward factors of ½ and 2 in various rows and columns are avoided.

A so-called especially orthotropic lamina is an orthotropic lamina whose principal material axes are aligned with the natural body axes:

©IJRASET 2015: All Rights are Reserved

Volume 3 Issue VII, July 2015
ISSN: 2321-9653
International Journal for Research in Applied Science & Engineering Technology (IJRASET)

$$\begin{bmatrix}\sigma_x\\ \sigma_y\\ \tau_{xy}\end{bmatrix} = \begin{bmatrix}\sigma_1\\ \sigma_2\\ \tau_{12}\end{bmatrix} = \begin{bmatrix}Q_{11} & Q_{12} & 0\\ Q_{12} & Q_{22} & 0\\ 0 & 0 & Q_{66}\end{bmatrix}\begin{bmatrix}\varepsilon_1\\ \varepsilon_2\\ \gamma_{12}\end{bmatrix} \quad \ldots\ldots\ldots\ldots(24)$$

where the principal material axes are shown in fig. 2. These stress-strain relations were introduced before and apply when the principal material directions of an orthotropic lamina are used as coordinates. Principal material coordinates do not coincide with the natural coordinates of the body after it is constructed. Thus the laminate loses its pure orthotropic characteristics and becomes an orthotropic material in an unnatural manner. This means fiber coordinate is at different angle other than principal material coordinate system. Then, the basic question is: given the stress-strain relations in the principal material coordinates, what are the stress-strain relations in x-y coordinates? Accordingly, we use the stress and strain transformations of equations (18) and (19) along with Reuter's matrix, eq. (21), after abbreviating eq. (24) as

$$\begin{bmatrix}\sigma_1\\ \sigma_2\\ \tau_{12}\end{bmatrix} = [Q]\begin{bmatrix}\varepsilon_1\\ \varepsilon_2\\ \gamma_{12}\end{bmatrix} \quad \ldots\ldots\ldots\ldots(25)$$

to obtain

$$\begin{bmatrix}\sigma_x\\ \sigma_y\\ \tau_{xy}\end{bmatrix} = [T]^{-1}\begin{bmatrix}\sigma_1\\ \sigma_2\\ \tau_{12}\end{bmatrix} = [T]^{-1}[Q][R][T][R]^{-1}\begin{bmatrix}\varepsilon_x\\ \varepsilon_y\\ \gamma_{xy}\end{bmatrix} \quad \ldots\ldots\ldots(26)$$

However, $[R][T][R]^{-1}$ can be shown to be $[T]^{-T}$ where the superscript T denotes the matrix transpose. Then, if we use the abbreviation

$$\overline{[Q]} = [T]^{-1}[Q]\,[T]^{-T} \quad \ldots\ldots\ldots\ldots(27)$$

the stress-strain relations in x-y coordinates are

$$\begin{bmatrix}\sigma_x\\ \sigma_y\\ \tau_{xy}\end{bmatrix} = \overline{[Q]}\begin{bmatrix}\varepsilon_x\\ \varepsilon_y\\ \gamma_{xy}\end{bmatrix} = \begin{bmatrix}\overline{Q_{11}} & \overline{Q_{12}} & \overline{Q_{16}}\\ \overline{Q_{12}} & \overline{Q_{22}} & \overline{Q_{26}}\\ \overline{Q_{16}} & \overline{Q_{26}} & \overline{Q_{66}}\end{bmatrix}\begin{bmatrix}\varepsilon_x\\ \varepsilon_y\\ \gamma_{xy}\end{bmatrix} \quad \ldots\ldots\ldots(28)$$

in which

$$\overline{Q_{11}} = Q_{11}\cos^4\theta + 2(Q_{12} + 2Q_{66})\sin^2\theta\cos^2\theta + Q_{22}\sin^4\theta$$

$$\overline{Q_{12}} = (Q_{11} + Q_{22} - 4Q_{66})\sin^2\theta\cos^2\theta + Q_{12}(\sin^4\theta + \cos^4\theta)$$

$$\overline{Q_{22}} = Q_{11}\sin^4\theta + 2(Q_{12} + 2Q_{66})\sin^2\theta\cos^2\theta + Q_{22}\cos^4\theta \qquad (4.85)$$

$$\overline{Q_{16}} = (Q_{11} - Q_{12} - 2Q_{66})\sin\theta\cos^3\theta + (Q_{11} - Q_{12} + 2Q_{66})\sin^3\theta\cos\theta$$

$$\overline{Q_{26}} = (Q_{11} - Q_{12} - 2Q_{66})\sin^3\theta\cos\theta + (Q_{12} - Q_{22} + 2Q_{66})\sin\theta\cos^3\theta$$

$$\overline{Q_{66}} = (Q_{11} + Q_{22} - 2Q_{12} - 2Q_{66})\sin^2\theta\cos^2\theta + Q_{66}(\sin^4\theta + \cos^4\theta)$$

where the bar over the $\overline{Q_{ij}}$ matrix denotes that we are dealing with the transformed reduced stiffnesses instead of the reduced stiffnesses, $\overline{Q_{ij}}$.

As an alternative to the foregoing procedure, we can express the strains in terms of the stresses in body coordinates by either (1) inversion of the stress-strain relation in eq. (27) or (2) transformation of the strain-stress relations in principal material coordinates from eq. (5),

$$\begin{bmatrix}\varepsilon_1\\ \varepsilon_2\\ \gamma_{12}\end{bmatrix} = \begin{bmatrix}S_{11} & S_{12} & 0\\ S_{12} & S_{11} & 0\\ 0 & 0 & S_{66}\end{bmatrix}\begin{bmatrix}\sigma_1\\ \sigma_2\\ \tau_{12}\end{bmatrix} \quad \ldots\ldots\ldots(29)$$

©IJRASET 2015: All Rights are Reserved

Volume 3 Issue VII, July 2015
ISSN: 2321-9653
International Journal for Research in Applied Science & Engineering Technology (IJRASET)

to body coordinates. We choose the second approach and apply the transformations of Equations (18) and (19) along with Reuter's matrix, eq. (21), to obtain

$$\begin{bmatrix}\varepsilon_x\\ \varepsilon_y\\ \gamma_{xy}\end{bmatrix} = [T]^T[S][T]\begin{bmatrix}\sigma_x\\ \sigma_y\\ \tau_{xy}\end{bmatrix} = \begin{bmatrix}\overline{S_{11}} & \overline{S_{12}} & \overline{S_{16}}\\ \overline{S_{12}} & \overline{S_{22}} & \overline{S_{26}}\\ \overline{S_{16}} & \overline{S_{26}} & \overline{S_{66}}\end{bmatrix}\begin{bmatrix}\sigma_x\\ \sigma_y\\ \tau_{xy}\end{bmatrix} \quad \ldots\ldots\ldots\ldots (30)$$

where $[R][T]^{-1}[R]^{-1}$ was found to be$[T]^T$ and

$$\overline{S_{11}} = S_{11}\cos^4\theta + (2S_{12} + S_{66})\sin^2\theta\cos^2\theta + S_{22}\sin^4\theta$$

$$\overline{S_{12}} = S_{12}(\sin^4\theta + \cos^4\theta) + (S_{11} + S_{22} - S_{66})\sin^2\theta\cos^2\theta +$$

$$\overline{S_{22}} = S_{11}\sin^4\theta + (2S_{12} + S_{66})\sin^2\theta\cos^2\theta + S_{22}\cos^4\theta$$

$$\overline{S_{16}} = (2S_{11} - 2S_{12} - S_{66})\sin\theta\cos^3\theta - (2S_{22} - 2S_{12} - S_{66})\sin^3\theta\cos\theta$$

$$\overline{S_{26}} = (2S_{11} - 2S_{12} \quad (31) \qquad)\cos\theta - (2S_{22} - 2S_{12} - S_{66})\sin\theta\cos^3\theta$$

$$\overline{S_{66}} = 2(2S_{11} + 2Q_{22} - 4S_{12} - S_{66})\sin^2\theta\cos^2\theta + S_{66}(\sin^4\theta + \cos^4\theta)$$

Recall that the Sij are defined in terms of the engineering constants in eq. (6).

Because of the presence of $\overline{Q_{11}}$ and $\overline{Q_{66}}$ in eq. (28) and of S16 and S26 in eq. (30), the solution of problems involving so-called generally orthotropic lamina is more difficult than problems with so-called especially orthotropic lamina. That is, difficult than problems with so-called especially orthotropic lamina. That is, shear-extension coupling complicates the solution of problems. As a matter of fact, there is no difference between solutions for generally orthotropic lamina whose stress-strain relations, under conditions of plane stress, can be written as

$$\begin{bmatrix}\sigma_1\\ \sigma_2\\ \tau_{12}\end{bmatrix} = \begin{bmatrix}Q_{11} & Q_{12} & Q_{16}\\ Q_{12} & Q_{22} & Q_{26}\\ Q_{16} & Q_{26} & Q_{66}\end{bmatrix}\begin{bmatrix}\varepsilon_1\\ \varepsilon_2\\ \gamma_{12}\end{bmatrix} \quad \ldots\ldots\ldots\ldots (32)$$

or in inverted from as

$$\begin{bmatrix}\varepsilon_1\\ \varepsilon_2\\ \gamma_{12}\end{bmatrix} = \begin{bmatrix}S_{11} & S_{12} & S_{16}\\ S_{12} & S_{22} & S_{26}\\ S_{16} & S_{26} & S_{66}\end{bmatrix}\begin{bmatrix}\sigma_1\\ \sigma_2\\ \tau_{12}\end{bmatrix} \quad \ldots\ldots\ldots (33)$$

where the anisotropic compliances in terms of the engineering constants are

$$S_{11} = \frac{1}{E_1} \qquad S_{22} = \frac{1}{E_2} \qquad S_{16} = \frac{\eta_{12,1}}{E_1} = \frac{\eta_{1,12}}{G_{12}}$$

$$S_{12} = -\frac{\nu_{12}}{E_1} = -\frac{\nu_{21}}{E_2} \qquad S_{66} = \frac{1}{G_{12}} \qquad S_{26} = = \frac{\eta_{12,2}}{E_2} = \frac{\eta_{2,12}}{G_{12}} \qquad (34)$$

Note that some new engineering constants have been used. The new constants are called coefficients of mutual influence by Lekhnistskii and are defined as

ηi, ij = coefficient of mutual influence of the first kind that characterizes stretching in the i-direction caused by shear stress in the ij-plane

$$\eta_{i,ij} = \frac{\varepsilon_i}{\gamma_{ij}} \quad \ldots\ldots\ldots\ldots\ldots (35)$$

for $\tau_{ij} = \tau$ and all other stresses are zero.

ηij, i = coefficient of mutual influence of the second kind characterizing shearing in the ij-plane caused by normal stress in the i-direction

$$\eta_{ij,i} = \frac{\gamma_{ij}}{\varepsilon_i} \quad \ldots\ldots\ldots\ldots\ldots (36)$$

©IJRASET 2015: All Rights are Reserved

for $\sigma_i = \sigma$ and all other stresses are zero.

Coefficients of mutual influence and the Poisson's ratio those are defined by Lekhnitskii are reversed in subscripts from the present notation. As Poisson's ratios can also be called coefficients of mutual influence, these have not been named very effectively. More appropriate way to call shear-extension coupling coefficients are ηij, i and ηi, ij.

To define Chentsov coefficients other anisotropic elasticity relations which are used are shearing stresses and shearing strains. However lamina under plane stress are no affected by Chentsov coefficients because the coefficients are related to S45, S46, and S56. The Chentsov coefficients are defined as

μij, kl = Chentsov coefficient that characterizes shearing strain in the kl-plane due to shearing stress in the ij-plane. i.e.,

$$\mu_{ij,kl} = \frac{\gamma_{kl}}{\gamma_{ij}} \qquad \ldots\ldots\ldots\ldots\ldots\ldots (37)$$

for $\tau_{ij} = \tau$ and all other stresses are zero.

The Chentsov coefficients are subject to the reciprocal relations

$$\frac{\mu_{kl,ij}}{G_{kl}} = \frac{\mu_{ij,kl}}{G_{ij}} \qquad \ldots\ldots\ldots\ldots\ldots\ldots (38)$$

Note that the Chentsov coefficients are more effectively called the functional name of shear-shear coupling coefficients.

The out-of-plane shearing strains of an anisotropic lamina due to in-plane shearing stress and normal stresses are

$$\gamma_{13} = \frac{\eta_{1,13}\sigma_1 + \eta_{2,13}\sigma_2 + \mu_{12,13}\tau_{12}}{G_{13}}$$

$$\gamma_{23} = \frac{\eta_{1,23}\sigma_1 + \eta_{2,23}\sigma_2 + \mu_{12,23}\tau_{12}}{G_{23}} \qquad (39)$$

Here the required coupling coefficients are shear-shear coupling coefficients and the shear-extension coupling coefficients. Unless an orthotropic material is stressed in coordinates other than the principal material coordinates neither of these shear strains are aroused. In such cases we can obtain the shear-shear coupling coefficients and the shear-extension coupling coefficients from the transformed compliances as in the following paragraph.

Compare the transformed orthotropic compliances in eq. (31) with the anisotropic compliances in terms of engineering constants in eq. (34). Obviously an apparent shear-extension coupling coefficient results when an orthotropic lamina is stresses in non-principal material coordinates. Redesignate the coordinates 1 and 2 in eq. (33) as x and y because, by definition, an anisotropic material has no principal material directions. Then, substitute the redesignated Sij from eq. (34) in eq. (31) along with the orthotropic compliances in eq. (6). Finally, the apparent engineering constants for an orthotropic lamina that is stressed in non-principal x-y coordinates are

$$\frac{1}{E_x} = \frac{1}{E_1}\cos^4\theta + \left[\frac{1}{G_{12}} - \frac{2\nu_{12}}{E_1}\right]\sin^2\theta\cos^2\theta + \frac{1}{E_2}\sin^4\theta$$

$$\nu_{xy} = E_x\left[\frac{\nu_{12}}{E_1}(\sin^4\theta + \cos^4\theta) - \left[\frac{1}{E_1} + \frac{1}{E_2} - \frac{1}{G_{12}}\right]\sin^2\theta\cos^2\theta\right]$$

$$\frac{1}{E_y} = \frac{1}{E_1}\sin^4\theta + \left[\frac{1}{G_{12}} - \frac{2\nu_{12}}{E_1}\right]\sin^2\theta\cos^2\theta + \frac{1}{E_2}\cos^4\theta$$

$$\frac{1}{G_{xy}} = 2\left[\frac{2}{E_1} + \frac{2}{\Gamma} + \frac{4\nu_{12}}{\Gamma} - \frac{1}{\hat{\ }_2}\right]\sin^2\theta\cos^2\theta + \frac{1}{G_{12}}(\sin^4\theta + \cos^4\theta)$$

---40

$$\eta_{xy,\,x} = E_x\left[\left[\frac{2}{E_1} + \frac{2\nu_{12}}{E_1} - \frac{1}{G_{12}}\right]\sin\theta\cos^3\theta - \left[\frac{2}{E_2} + \frac{2\nu_{12}}{E_1} - \frac{1}{G_{12}}\right]\sin^3\theta\cos\theta\right]$$

$$\eta_{xy,\,y} = E_y\left[\left[\frac{2}{E_1} + \frac{2\nu_{12}}{E_1} - \frac{1}{G_{12}}\right]\sin^3\theta\cos\theta - \left[\frac{2}{E_2} + \frac{2\nu_{12}}{E_1} - \frac{1}{G_{12}}\right]\sin\cos^3\theta\right]$$

©IJRASET 2015: All Rights are Reserved

Volume 3 Issue VII, July 2015
ISSN: 2321-9653
International Journal for Research in Applied Science & Engineering Technology (IJRASET)

Now, for a given number of lamina and their stacking sequence, mechanical properties of lamina (Young Modulus, Shear modulus and Poisson's ratio) along global coordinates (x, y and z) can be calculated from their corresponding mechanical properties along lamina coordinates using equations 3.97. Then the equivalent mechanical properties of the all the lamina together i.e whole the object made out of all the required lamina is calculated by finding out the modified stiffness matrix $\bar{Q}$ by using equation 3.85 and finding out also the in-plane stiffness coupling matrix [A], bending-stretching coupling [B] and bending stiffness coupling [D] by the following equations.

$$[A] = \sum_{k=1}^{n} [\bar{Q}]^k (z_k - z_{k-1})$$

$$] = \frac{1}{2} \sum_{k=1}^{n} [\bar{Q}]^k (z_k^2 - z_{k-1}^2) \quad \text{-------- (41)}$$

$$[D] = \frac{1}{3} \sum_{k=1}^{n} [\bar{Q}]^k (z_k^3 - z_{k-1}^3)$$

Where, z is the layer thickness and k is the layer number.
Mechanical properties of each layer along global coordinate and equivalent mechanical properties of whole the body have been calculated by MATLAB through a M Program

II. GEOMETRY AND PARAMETERS OF THE UNIFORM DRIVE SHAFT MADE OF COMPOSITE MATERIAL

A drive shaft of OD 90mm and thickness 2.04 mm has been considered for analysis. Length of the drive shaft is 1250mm. It is made out of a composite material High Strength Carbon/ Epoxy. Property of the HS Carbon/Epoxy has been presented below.

Table 1: Property of the HS Carbon/Epoxy.

E11	E22	G12	ν12	Yield Strength	ρ
134 GPa	7.0 GPa	7.0 GPa	0.3	440 MPa	1600 kg/m3

The composite drive shaft has been made with 17 layer each of having thickness 0.12mm and stacking sequence [-56°/-51°/74°/-82°/67°/70°/13°/-44°/-75°]s.
After putting the value of E11, E22, G12 and ν12 in MATLAB program shown in appendix A we get lamina-wise mechanical properties have been shown in table 2. To calculate lamina wise properties equations 40 have been used.

Table 2: Mechanical properties of each lamina of composite.

Lamina no.	θ	Exy (GPa)	Exz (GPa)	Eyz (GPa)	νxy	νyz	νzx	Gxy (GPa)	Gxz (GPa)	Gyz (GPa)
1	-56°	9.5872	18.6615	18.6615	0.0578	0	0	6.3585	6.3585	6.3585
2	-51°	10.7011	15.3143	15.3143	0.0690	0	0	6.4284	6.4284	6.4284
3	74°	7.4734	52.6700	52.6700	0.0260	0	0	5.9713	5.9713	5.9713
4	-82°	7.1139	95.9714	95.9714	0.0183	0	0	5.8454	5.8454	5.8454
5	67°	8.0344	32.8814	32.8814	0.0363	0	0	6.1238	6.1238	6.1238
6	70°	7.7616	39.8081	39.8081	0.0315	0	0	6.0556	6.0556	6.0556
7	13°	65.9614	7.3072	7.3072	0.2035	0	0	5.9162	5.9162	5.9162
8	-44°	12.9540	12.2068	12.2068	0.0860	0	0	6.4592	6.4592	6.4592
9	-75°	7.4135	56.7105	56.7105	0.0248	0	0	5.9520	5.9520	5.9520

To calculate mechanical properties of composite material High Module Carbon/ Epoxy first coupling matrices (stiffness coupling matrix [A], bending-stretching coupling [B] and bending stiffness coupling [D]) have been calculated from equation 41 with help of a MATLAB program shown in appendix B. The program gives the following result.

©IJRASET 2015: All Rights are Reserved

Volume 3 Issue VII, July 2015
ISSN: 2321-9653
International Journal for Research in Applied Science & Engineering Technology (IJRASET)

Table 3: Mechanical properties of whole the composite.

Exy (GPa)	Exz (GPa)	Eyz (GPa)	vxy	vyz	vzx	Gxy (GPa)	Gxz (GPa)	Gyz (GPa)
26.6893	71.6799	71.6799	0.2090	0	0	20.0170	20.0170	20.0170

Above calculation for composite property has been done in MATLAB R10 and it agrees with the result derived from calculation mentioned in Ref. [9] which has been done by Genetic Algorithm. The result from Ref [9] has been shown below.

Material	E_x (MPa)	E_y (MPa)	G_{xy} (MPa)	ν_{12}
E-Glass/Epoxy	28.99	20.69	9.94	0.35
HS Carbon/Epoxy	26.69	71.68	20.02	0.2
HM Carbon/Epoxy	40.69	62.14	34.20	0.39

Fig 6: Result from Reference [9]

```
MATLAB desktop keyboard shortcuts, such as Ctrl+S, are now customizable.
In addition, many keyboard shortcuts have changed for improved consistency
across the desktop.

To customize keyboard shortcuts, use Preferences. From there, you can also
restore previous default settings by selecting "R2009a Windows Default Set"
from the active settings drop-down list. For more information, see Help.

Click here if you do not want to see this message again.


MP =

   26.6893   71.6799   20.0170    0.5503    0.2090

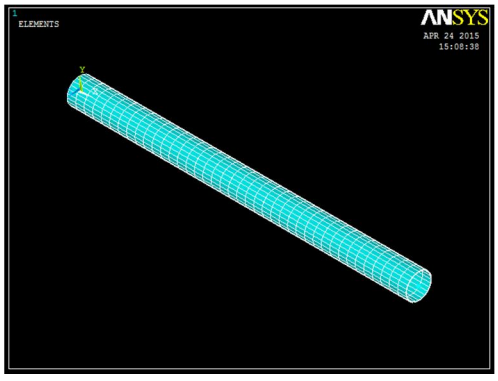

MP =

    9.5872   18.6615    6.3585    0.0578
   10.7011   15.3143    6.4284    0.0690
    7.4734   52.6700    5.9713    0.0260
    7.1139   95.9714    5.8454    0.0183
    8.0344   32.8814    6.1238    0.0363
    7.7616   39.8081    6.0556    0.0315
   65.9614    7.3072    5.9162    0.2035
   12.9540   12.2068    6.4592    0.0860
    7.4135   56.7105    5.9520    0.0248
```

Fig 7: Result from Matlab R10 used in this work.

To validate the FEA model work of Sanjay Gumandi and Jagadeesh Kumar Akula as mentioned in reference [9] has been reproduced. Sanjay et. al. have used SHELL99 in ANSYS to analyze composite drive shaft of above mentioned dimension under a torsional load. Here in this project SOLID46 has been used instead of SHELL99 and same result has been arrived.

Modeling and Meshing of composite drive shaft have been done through an ANSYS APDL programming which has been produced in appendix C. Meshed model of uniform composite driveshaft as per the ANSYS APDL program has been shown below.



©IJRASET 2015: All Rights are Reserved

Volume 3 Issue VII, July 2015
ISSN: 2321-9653
International Journal for Research in Applied Science & Engineering Technology (IJRASET)

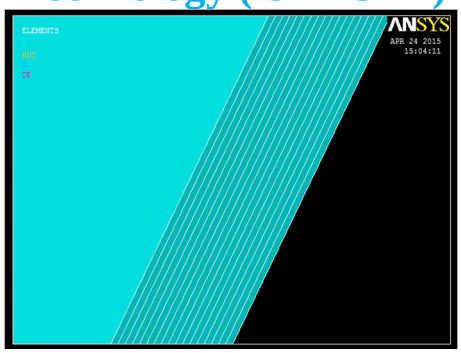


Fig. 8: Meshed model of composite drive shaft.

Here investigation has been done on composite drive shaft made of High Module Carbon/ Epoxy which has been imposed of torque 3500Nm (as per Gummandi Sanjay & Akula Jagadeesh Kumar et. al. [9]). To impose torque on each nodes of drive shaft FEA model MASS21 element has been introduced. Figure bellow depicts the Boundary Conditions and Loading of composite drive shaft.

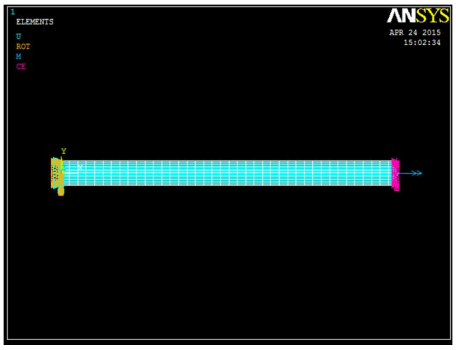


Fig. 9: Boundary Conditions and Loading.

Shaft has been fixed with all boundary conditions zero at one end and torque has been imposed on the other end. After imposing boundary conditions and loading model has been solved for the static loading.

After solution rotational deflection has been evaluated as 0.10368° which agree very much with the result of Sanjay et. al. [9]. Deflection result has been shown below.

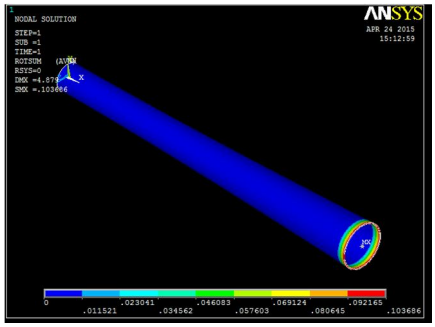


Fig. 10: Torsional deflection about axis of composite shaft as per this work.

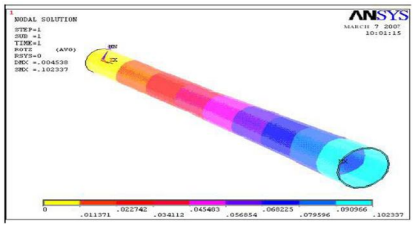


Fig. 11: Torsional deflection about axis of composite shaft as per Ref. [9].

As it has been mentioned above that layered composite drive shaft has yield strength 440 MPa so the Von-Mises stress should come below 440 MPa. Figure below shows the Von-Mises stress distribution of composite drive shaft.

As per the figure it is clear that equivalent stress or Von-Mises stress is 350.927 MPa which is well below the value of yield strength

©IJRASET 2015: All Rights are Reserved

Volume 3 Issue VII, July 2015
ISSN: 2321-9653
International Journal for Research in Applied Science & Engineering Technology (IJRASET)

(440 MPa) after imposing the limiting torque value of 3500 Nm. So the model of composite drive shaft has been validated.

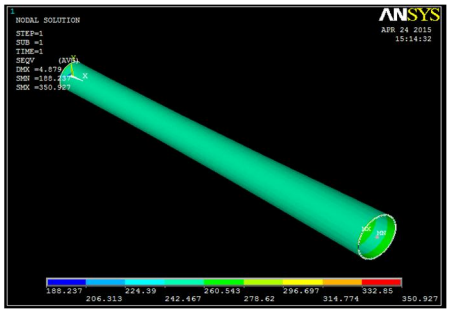


Fig. 12: Torsional deflection of composite shaft.

Now in the next chapter design of composite drive shaft would be modified and would be investigated with help of ANSYS whether the modification can withstand the limiting torque i.e. 3500 Nm or not.

III. MODAL ANALYSIS OF THE SHAFT

Another analysis has been done on this composite drive shaft is the Modal analysis. By this analysis natural frequency of the shaft has been found out up to three modes.

Below are the figures for 1st, 2nd and 3rd mode vibration.

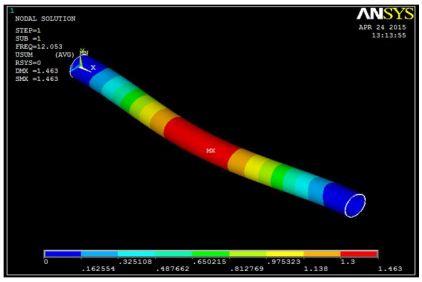


Fig. 13: 1st mode vibration.

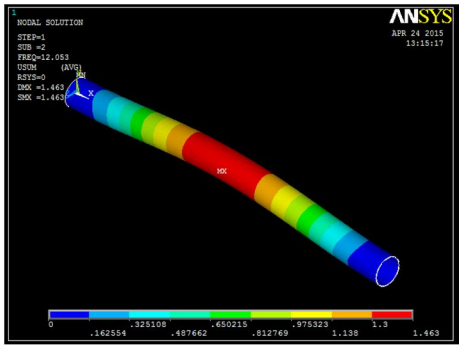


Fig. 14: 2nd mode vibration.

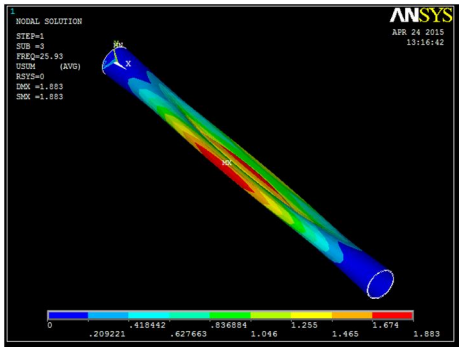


Fig. 15: 3rd mode vibration.

©IJRASET 2015: All Rights are Reserved

Frequencies for three modes have been shown in the table below.

***** INDEX OF DATA SETS ON RESULTS FILE *****

SET	TIME/FREQ	LOAD STEP	SUBSTEP	CUMULATIVE
1	12.053 Hz	1	1	1
2	12.053 Hz	1	2	2
3	25.930 HZ	1	3	3

Fig 16: Figure from ANSYS result depiting Frequencies of the composite drive shaft at different modes of vibration.

It is clear from the above figures that the drive shaft will collapse on 3rd mode of vibration.

IV. DESIGN MODIFICATIONS ADPOTED

In the base paper reference [9] static and modal analysis of such a drive shaft has been performed which is dimensionally uniform. In this chapter an idea of tapered drive shaft has been adopted. Static and modal analyses of a tapered drive shaft of different taper angles have been performed in this chapter.

Behind this idea the main reason is that a taper beam always exhibits lower stress than a uniform beam. To perform the static and modal analysis of a taper beam two taper angles have been taken. These two angles are 1° and 1.5°.

When we consider 1° the dimensions of the drive shaft becomes as follows.

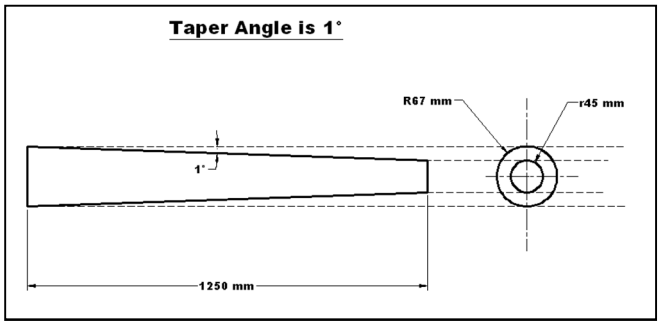


Fig 17: Geometry of a tapered drive shaft having taper angle 1°.

The analysis has been done in FEA software called ANSYS. Geometry of the above figure that appears in the ANSYS GUI has been shown below.

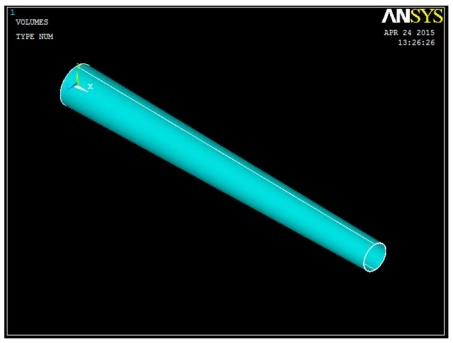


Fig 18: Geometry of a tapered drive shaft having taper angle 1° shown in ANSYS.

After generating geometry and meshing it in ANSYS, it has been simulated for a torque of 3500 Nm. Material used for this drive shaft is HM Carbon/Epoxy. An APDL program has been used for generating geometry, meshing it and imposing boundary conditions C.

After solving under the given load and boundary conditions following results have been derived.

First vector sum of rotational deflection has been calculated due to the above torque at different sections of the drive shaft.

Then Von-Misses stress has been calculated for different sections of the tapered drive shaft.

Results of the above investigations have been presented in the figures below.

©IJRASET 2015: All Rights are Reserved

Volume 3 Issue VII, July 2015
ISSN: 2321-9653
International Journal for Research in Applied Science & Engineering Technology (IJRASET)

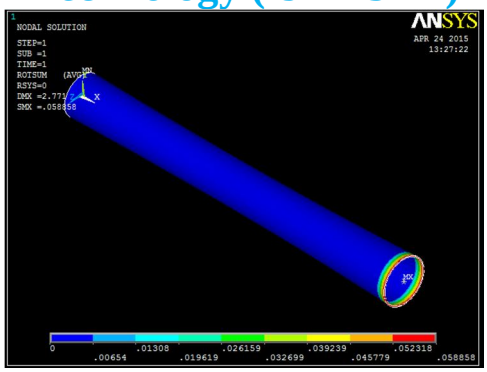


Fig 19: Vector sum of rotational deflection of taped shaft with taper angle 1°.

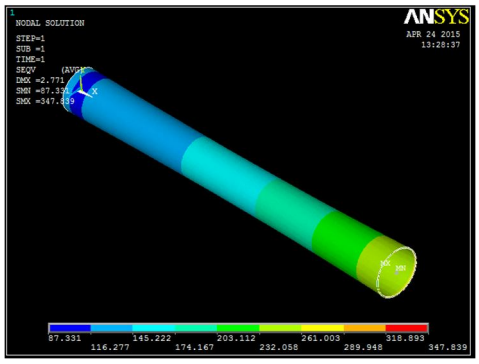


Fig 20: Von-Misses stress of the tapered shaft with taper angle 1°.

It is clear from the above figure that deflection and Von-Misses stress of the tapered drive shaft with taper angle 1° are of lesser value. Rotational vector sum of the uniform drive shaft with same torque load is 0.103686° but in case of the tapered drive shaft with taper angle 1° is 0.058858°.

Similarly Von-Misses stress of the uniform drive shaft is 350.927 N/mm2 which is larger than the value of Von-Misses stress of tapered shaft which is 347.839 N/mm2. After analyzing static analysis of the tapered shaft under torque load of 3500 Nm, Modal analysis has been done on the taper shaft. Figure below represents the result calculated from the modal analysis.

***** INDEX OF DATA SETS ON RESULTS FILE *****

SET	TIME/FREQ	LOAD STEP	SUBSTEP	CUMULATIVE
1	14.517	1	1	1
2	14.517	1	2	2
3	17.204	1	3	3

Fig 21: Frequencies of the tapered drive shaft at different modes of vibration.

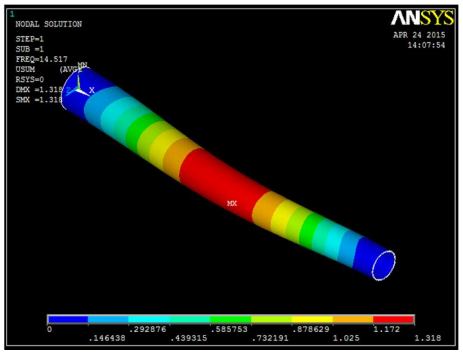


Fig 22: Deflection of shaft under 1st mode of vibration.

©IJRASET 2015: All Rights are Reserved

Volume 3 Issue VII, July 2015
ISSN: 2321-9653
International Journal for Research in Applied Science & Engineering Technology (IJRASET)

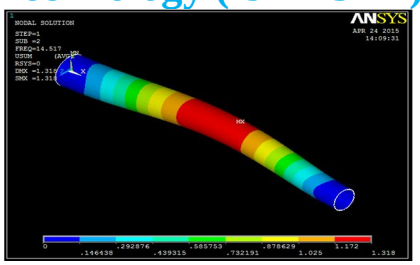


Fig 23: Deflection of shaft under 2nd mode of vibration.

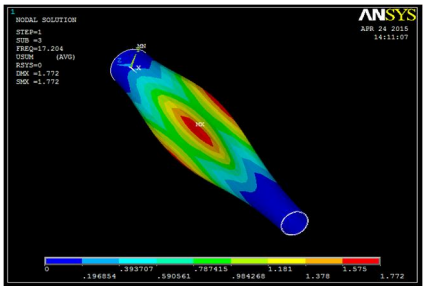


Fig 24: Deflection of shaft under 3rd mode of vibration.

After analyzing the tapered drive shaft with taper angle 1°, now taper angle has been increased to 1.5° and all the results have been represented below.

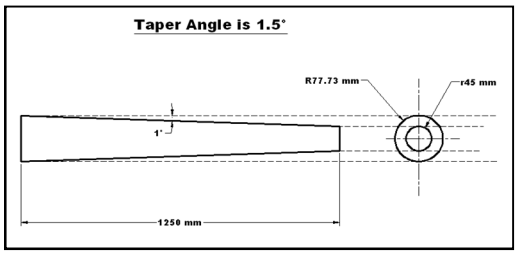


Fig 25: Geometry of a tapered drive shaft having taper angle 1.5°.

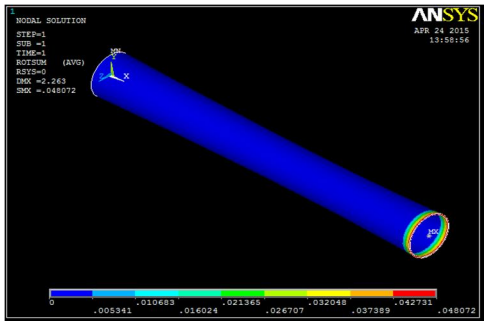


Fig 26: Vector sum of rotational deflection of taped shaft with taper angle 1.5°.

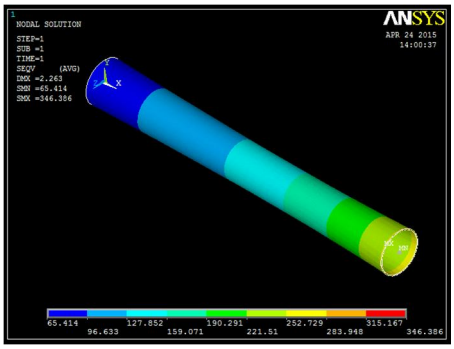


Fig 27: Von-Misses stress of the tapered shaft with taper angle 1.5°.

©IJRASET 2015: All Rights are Reserved

Volume 3 Issue VII, July 2015
ISSN: 2321-9653
International Journal for Research in Applied Science & Engineering Technology (IJRASET)

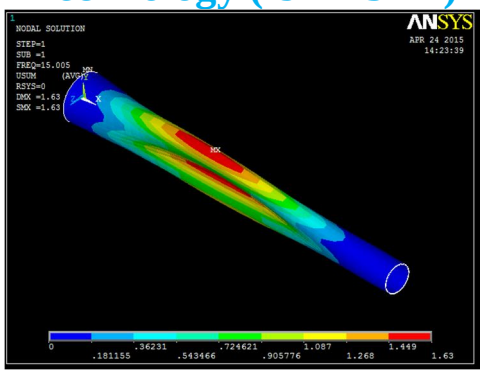


Fig 28: Deflection of 1.5 °taper shaft under 1st mode of vibration.

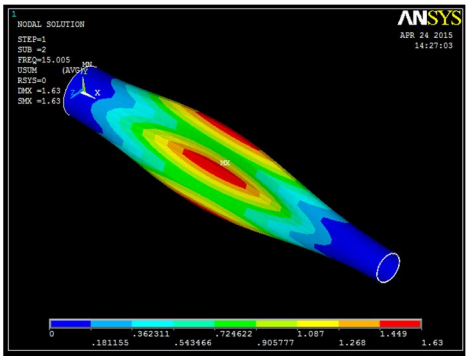


Fig 29: Deflection of 1.5 °taper shaft under 2nd mode of vibration.

```
*****  INDEX OF DATA SETS ON
     RESULTS FILE  *****

SET   TIME/FREQ    LOAD STEP
     SUBSTEP  CUMULATIVE
   1  15.005              1
        1          1
   2  15.005              1
```

Table 30: Frequencies of the 1.5° tapered drive shaft at different modes of vibration.

V. RESULT AND DISCUSSION

Parameters	Uniform Shaft	1° Taper	1.5° Taper
Rotational Deflection	0.103686 Degree	0.058858 Degree	0.048072 Degree
Von-Misses Stress	350.927 N/mm2	347.839 N/mm2	346.386 N/mm2

From the above study it is clear that tapered drive shaft exhibits lesser deflection and less Von-Misses stress under a given torque. But with increase of taper angle it shows some instability under vibration. So it is a matter of further research to find out optimized taper angle so that natural frequencies in different modes remains as low as possible.

From the research made in this work a conclusion may be drawn that any other profile than the conventional uniform cylindrical profile can also be used as transmission shaft. In this work instead of an isotropic material like steel, a composite material used which is orthotropic in character. Same torque has been imposed on an uniform drive shaft and on a tapered drive shaft made of High Module Carbon/Epoxy composite material. From the result it is clear that in tapered drive shaft less stress is created due to same torque as applied on uniform drive shaft. But a problem is there as tapered drive shaft is more vulnerable under vibration because tapered drive shaft shows more natural frequency than uniform drive shaft.

It has been clearly proved from this work that induced stress in the tapered drive shaft decreases with increase in taper angle of shaft but natural frequency also increases with increase of taper angle which makes the concept unacceptable. Because, increase in natural

©IJRASET 2015: All Rights are Reserved

frequency makes the design vulnerable under vibration.

So it is a matter of further research to find out optimal taper angle so that stress as well as natural frequency both can be reduced.

REFERENCES

[1] Fredrik Cato, Magnus Taskinen "Noise and Vibration Investigation of Composite Shaft", A Master Degree Thesis, Department of Mechanical Engineering, University of Kralskrona, Sweden, 1998;

[2] S.Rajendran and D.Q.Song, "Finite Element Modelling of Delamination Buckling of Composite Panel Using ANSYS", Proceedings of 2nd Asian ANSYS User Conference, Nov 11-13, 1998, Singapore.

[3] Murat Ocalan, "High flexibility rotorcraft drive shaft using flexible matrix composites and active bearing control.", Master Degree Thesis, Department of Mechanical Engineering, The Pennsylvania State University, 2002.

[4] Tomas Zackrisson, "The Modeling and simulation of a driveline with an automatic gearbox", A Master Degree Thesis, Department of Mechanical Engineering, Royal Institute of Technology, 2003;

[5] T.Rangaswami, S.Vijayanarangan, R.A.Chandrashekhar, T.K.Venktesh and K.Anantharaman, "optimal design and analysis or automotive composite drive shaft." International Symposium of Research Student on Material Science and Engineering, 2002-2004 chennai.

[6] David B. Adams, "Optimization Frameworks for Discrete Composite Laminate Stacking Sequences", A Thesis for DOCTOR OF PHILOSOPHY, Virginia Polytechnic Institute and State University, 2005.

[7] Nicholas M. Northcote, "The Modeling and Control of an Automotive Drivetrain", A Master Degree Thesis, Department of Mechanical Engineering, University of Sellenbosch, 2006;

[8] Yeow Ng, Al Kumnick, "Determination of Cross-Ply Laminate Stacking Sequence for The Compression Strength Testing of A unidirectional Boron EPOXY material.", SAMPE Fall Technical conferences-Dallas, November 6-9, 2006 Dallas, TX.

[9] Gummandi Sanjay & Akula Jagadeesh Kumar, "Optimum Design and Analysis of a Composite Drive Shaft for an Automobile", Proceedings of the World Congress on Engineering 2008 Vol iii, WCE 2008, JANUARY 6 - 8, 2008, LONDON, U.K.

[10] Master Degree Thesis, Department of Mechanical Engineering, Blekinge Institute of Technology, Karlskrona, Sweden, 2007.

[11] Duncan J. Lawrie, "Development of a High Torque Density, Flexible, Composite Driveshaft", American Helicopter Society 63rd Annual Forum, Virginia Beach, VA, May 1-3, 2007.

[12] M.A.K. Chowdhuri, R.A. Hossain, "Design Analysis of an Automotive Composite Drive Shaft", International Journal of Engineering and Technology Vol.2(2), 2010, 45-48

[13] Matthew james vick, "Finite Element Study on the Optimization of an Orthotropic Composite Toroidal Shell" A Master Degree Thesis, School of Aerospace and Mechanical Engineering, University of Oklahoma, 2010

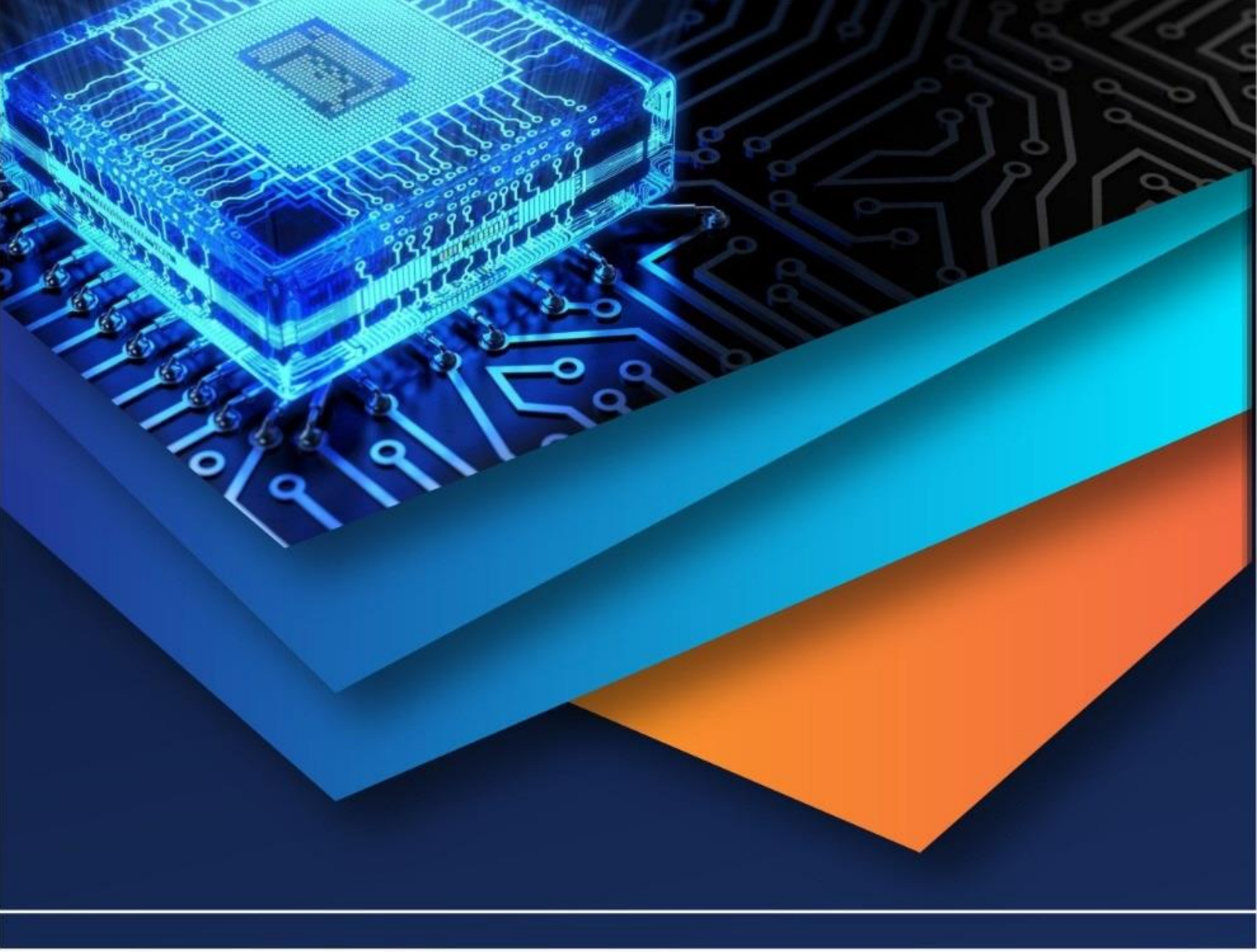
[14] Prof. George Z. Voyiadjis & Prof. Peter I. Kattan, "Mechanics of Composite Materials with MATLAB", Springer Publication.

[15] Robert M. Jones, "Mechanics of Composite Materials", Taylor & Francis, 2nd Edition.

[16] "The Focus", A Publication by "Phoenix Analysis & Design Technologies" (PADT) for ANSYS Users.

[17] A Tutorial on "Composite Analysis in ANSYS", ANSYS Inc.

©IJRASET 2015: All Rights are Reserved



10.22214/IJRASET

45.98

IMPACT FACTOR: 7.129

IMPACT FACTOR: 7.429

INTERNATIONAL JOURNAL FOR RESEARCH

IN APPLIED SCIENCE & ENGINEERING TECHNOLOGY

Call : 08813907089 (24*7 Support on Whatsapp)